Aksaray University
Journal of Science and Engineering
e-ISSN: 2587-1277
http://dergipark.gov.tr/asujse
http://asujse.aksaray.edu.tr

Aksaray J. Sci. Eng.
Volume **2,** Issue **2,** pp. **116-126**
doi: 10.29002/asujse.451444
Available online at DergiPark AKADEMİK

Research Article

The Electronic, Optical and Lattice Dynamical Properties of YIr_2X_2 (X=Si, Ge) Polymorphs: A DFT Study

Ahmet Bicer[1,*], Gokhan Surucu[2,3,4]

[1]Rectorate Central Unit, Burdur Mehmet Akif Ersoy University, Burdur 15030, Turkey
[2]Department of Electric and Energy, Ahi Evran University, Kırsehir 40100, Turkey
[3] Department of Physics, Middle East Technical University, Ankara 06800, Turkey
[4] Photonics Application and Research Center, Gazi University, Ankara 06500, Turkey

▪*Received Date: 06 Aug 2018* ▪*Revised Date: 15 Sep 2018* ▪*Accepted Date: 17 Sep 2018* ▪*Published Online: 26 Sep 2018*

Abstract

The electronic, optical, and lattice-dynamical properties of YIr_2X_2(X=Si, Ge) compounds are investigated using the first-principles plane-wave pseudopotential method within the GGA approximation. In particular, the lattice constant, density of state, dielectric constant, refractive index and phonon properties are calculated and discussed. The calculated lattice parameters are in good agreement with previous experimental and theoretical data, whereas the formation enthalpies of the compounds are -1.149 and -0.841 eV/f.u. indicating that the compounds are stable in the body-centered tetragonal structure. In addition, real and imaginary parts of the static dielectric constant are 52.26 and 72.68, respectively.

Keywords

Refractive Index, Dielectric Function, Phonon, Density Functional Theory.

1. INTRODUCTION

To date, large variety of ternary intermetallic systems have been discovered and many of them remain subjects of intensive scientific interest [1]. The broad family of 122-type intermetallic with a tetragonal $ThCr_2Si_2$ structure demonstrates a remarkable range of physical and chemical properties [2]. These systems include the ternary disilicide YIr_2Si_2, for which two superconducting polymorphic forms exist: a low-temperature modification (LT) with a

[*]**Corresponding Author:** Ahmet Bicer, ahmetbicer@mehmetakif.edu.tr

$ThCr_2Si_2$-type structure (T_c<2K) and high –temperature modification (HT) with a $CaBe_2Ge_2$-type structure (T_c~2.8 K) [3].

There are only experimental [1] study and a few theoretical [2-7] studies dealing with the structural, elastic, and electronic properties of tetragonal $ThCr_2Si_2$ structure, particularly YIr_2Si_2, in the literature. Especially, Valiska et al. have reported on existence of superconductivity in YIr_2Si_2 and $LaIr_2Si_2$ compounds in relation to crystal structure by experimental method [1]. Shein and Ivanovskii have investigated structural, electronic, elastic properties and chemical bonding in $LaNi_2P_2$ and $LaNi_2Ge_2$ by the first principles methods [2]. Stability, structural, elastic, and electronic properties of YIr_2Si_2 has been studied by Shein [3]. In addition, Shein and Ivanovskii [4-7] studied the structural, elastic, magnetic, and electronic properties of $SrPt_2As_2$, KCo_2Se_2, KFe_2AsSe, and $KFeAgTe_2$ polymorphs with $ThCr_2Si_2$-type structures by the first principles methods. Billington et al studied electron-phonon coupling and critical temperature in YIr_2Si_2 and $LaIr_2Si_2$ High-T_c superconducting polymorphs [8].

In this work, we aim to provide additional information to the existing data on the physical properties of YIr_2X_2(X= Si, Ge) polymorphs by using the first-principles plane wave pseudopotential method and we especially focus on the electronic, optical and lattice-dynamical. The obtained results are compared with previous theoretical calculations and available experimental findings. The layout of this paper is given as follows: the methodology is given in section 2; and the results and overall conclusion are presented and discussed in section 3.

2. MATERIALS AND METHOD

The calculations are performed by using the plane-wave pseudopotential (PP) approach to the density functional theory (DFT) by Cambridge Sequential Total Energy Package (CASTEP) code [9]. The electronic wave functions are obtained by using a density-mixing minimization method for the self-consistent field (SCF) calculation, and the structures are relaxed by using the Broyden, Fletcher, Goldfarb and Shannon (BFGS) method [10]. For the exchange and correlation terms in the electron–electron interaction, Perdew–Burke–Ernzerhof (PBE) type functional is used within the generalized gradient approximation (GGA) [11].

Atomic pseudopotentials are generated separately for atoms Y, Ir and Si by using the $4d^15s^2$, $5d^76s^2$ and $3s^23p^1$ atomic configurations, respectively. The tolerances for geometry optimization are set as the difference in total energy being within $5x10^{-6}$ eV/atom, the maximum ionic Hellmann–Feynman force within 0.01 eV/Å, the maximum ionic displacement within $5x10^{-4}$ Å, and the maximum stress within 0.02 GPa. The interactions between electrons and

core ions are simulated with separable Troullier-Martins [12] norm-conserving pseudopotentials. The wave functions are expanded in plane waves up to a kinetic-energy cutoff of 750 eV. This cut-off energy is determined to be adequate to study the investigated physical properties. Finally, the k-points of 10x10x4 which are generated by Monkhorst and Pack scheme are used for these compounds [13].

3. RESULTS AND DISCUSSIONS

3.1. Structural and Electronic Properties

In this work, YIr_2X_2 (X= Si, Ge) compounds crystallizes in the $ThCr_2Si_2$-type body centered tetragonal structure (space group *I4/mmm*; #139), which contains 10 atoms per unit cell. The unit cell of this compounds is shown in Fig. 1. Atomic positions for $ThCr_2Si_2$-type are Th:2a (0, 0, 0), Cr:4d (0,½, ¼), and Si:4e (0, 0, z_{Ch}), where z_{Ch} is the so-called internal coordinate [2].

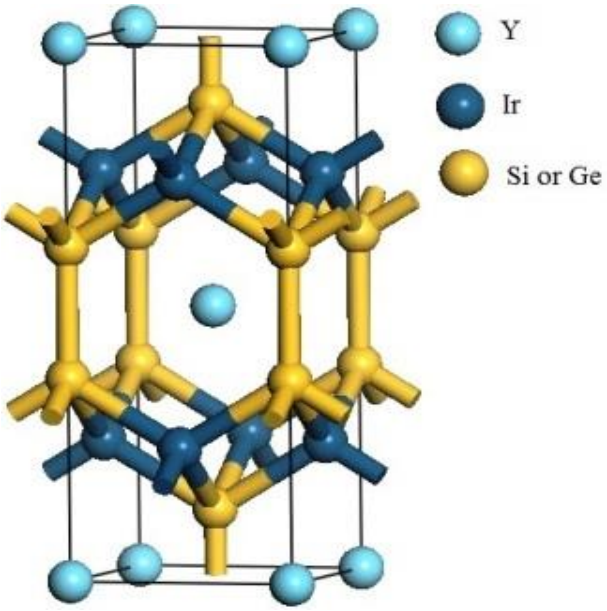

Figure 1. Crystal structure of YIr_2X_2 (X=Si, Ge) polymorphs.

As a first step, the equilibrium lattice parameters are optimized and their values are given in Table 1 along with the other theoretical and experimental data [1, 3]. The obtained results are in agreement with the other available values. The calculated lattice constants are higher (about 1%) than the experimental finding in Ref. [1] and roughly the same with the theoretical result in Ref. [3] for YIr_2Si_2 compound. We cannot make any comparisons for calculated properties of YIr_2Ge_2 because there are not available experimental and theoretical data in the literature. In addition, YIr_2Si_2 has similar properties with YIr_2Ge_2 compound.

Table 1. The calculated equilibrium lattice parameters (*a*, *c* in Å) and formation energies *(ΔH_f in eV/f.u.)*, for YIr_2X_2(X=Si, Ge) Polymorphs.

Compound	***a***	***c***	***ΔH_f***	***References***
YIr_2Si_2	4.080	10.051	-1.149	Present
	4.048	9.815		Exp. [1]
	4.0862	10.000		Theo. [2]
YIr_2Ge_2	4.160	10.334	-0.849	Present

We also calculated the formation energy (ΔH_f) for the YIr_2X_2 (X=Si, Ge) polymorphs using by the following common relation:

$$E_{form}^{YIr_2X_2} = E_{total}^{YIr_2X_2} - [E_{solid}^{Y} + 2E_{solid}^{Ir} + 2E_{solid}^{X}] \quad (1)$$

The calculated formation energies for YIr_2X_2 (X=Si, Ge) compounds are listed in Table 1. The negative formation energy value implies the structural stability of this compounds and confirming the electron numbers at Fermi levels listed in Table 2.

The band structures and corresponding partial density of states (PDOS) for these compounds along the high symmetry directions in the first Brillouin zone are calculated. Only the PDOS graphs are given in Fig. 2. For each compound, the PDOS reveals a metallic character. Furthermore, *d* orbital is seen to be the most dominant transitions, while s orbital is seen to be the weakest transitions.

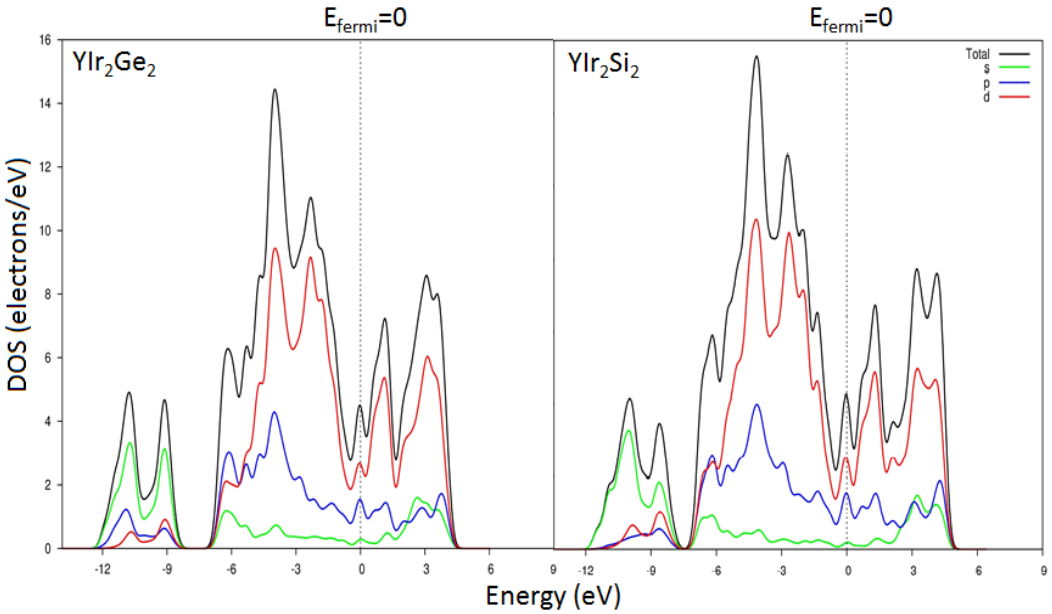

Figure 2. Calculated partial density of states (PDOS) of YIr_2X_2 (X=Si, Ge) polymorphs.

For the Band filling theory, if the numbers of bonding (anti-bonding) states increase (decrease), the stability of a material increases. Thus, the ratio W_{occ} (the width of the occupied states)/W_b (the width of the bonding states) may give information about the stability of the material. If the

value of this ratio is close to 1.0, the stability increases and also the distances from the bottom of the band to E_f and to the pseudogap W_p [14, 15]. In this paper, these parameters indicate structural stability and investigated parameters are given in Table 2 for YIr_2X_2 (X=Si, Ge). As can be seen from Table 2, W_{occ}/W_b values are very close to 1.0. On account of this, YIr_2X_2(X=Si, Ge) compounds seem to be stable.

Table 2. The calculated width of occupied states W_{occ} *(eV)*, bonding States W_b *(eV)*, pseudogap W_p and electron numbers at Fermi levels *n* (Fermi) for YIr_2X_2(X=Si, Ge) polymorphs.

Compound	W_{occ}	W_b	W_{occ}/W_b	W_P	***n***
YIr_2Si_2	12.389	11.914	1.039	-0.475	4.242
YIr_2Si_2	12.389	11.914	1.039	-0.475	4.242

3.2. Optical Properties

We now consider the optical properties for YIr_2X_2 (X=Si, Ge). The dielectric function ε(ω) can be used to describe the linear response of the system to electromagnetic radiation, which relates to the interaction of photons with electrons [16]. It is well known that the imaginary part $\varepsilon_2(\omega)$ of the dielectric function can be calculated with the momentum matrix elements between the occupied and unoccupied wave functions within the selection rules, and the real part $\varepsilon_1(\omega)$ and the imaginary part $\varepsilon_2(\omega)$ of the dielectric function follow the forms in equation (2) and (3), respectively. Other optical properties can be derived from the complex dielectric function. Expressions used for the dielectric functions, refractive index $n(\omega)$, and energy loss function $L(\omega)$ are given as follows [17-19]:

$$\varepsilon_1(\omega) = 1 + \frac{2}{\pi}\int_0^{\infty} \frac{\varepsilon_2(\omega')\omega' d\omega'}{\omega'^2 - \omega^2} \tag{2}$$

$$\varepsilon_2(\omega) = \frac{Ve^2}{2\pi \mathrm{h} m^2 \omega^2}\int d^2k \sum_{nn'} \left|\langle kn| p |kn'\rangle\right|^2 f(kn) \times \left[1 - f(kn')\right]\partial(E_{kn} - E_{kn'} - \mathrm{h}\omega) \tag{3}$$

where $\hbar\omega$ is the energy of the incident photon, p is the momentum operator, $\frac{\mathrm{h}}{i}\frac{\partial}{\partial x}$, $|kn\rangle$ is the eigenfunction with eigenvalue E_{kn} and $f(kn)$ is the Fermi distribution function.

$$n(\omega) = \frac{1}{\sqrt{2}}\left[\sqrt{\varepsilon_1^2(\omega) + \varepsilon_2^2(\omega)} + \varepsilon_1\right]^{1/2} \tag{4}$$

$$L(\omega) = -\mathrm{Im}\left(1/\varepsilon\right) = \varepsilon_2(\omega)/\left[\varepsilon_1^2(\omega) + \varepsilon_2^2(\omega)\right] \tag{5}$$

By using Equation (2)-(5), the real and imaginary parts of dielectric function ($\varepsilon_1(\omega)$, $\varepsilon_2(\omega)$), refractive index $n(\omega)$ and the energy loss function $L(\omega)$ are calculated [20]. The real and imaginary parts of dielectric function on the range of 0–10 eV for YIr_2X_2 (X=Si, Ge) are displayed in Figs.3 and 4, respectively.

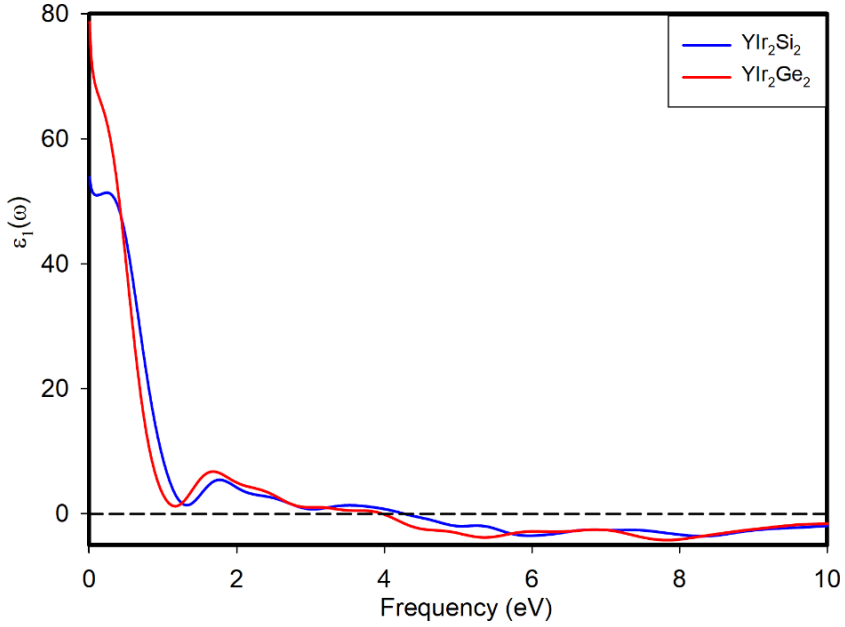

Figure 3. The real part $\varepsilon_1(\omega)$ of dielectric function of YIr_2X_2 (X=Si, Ge).

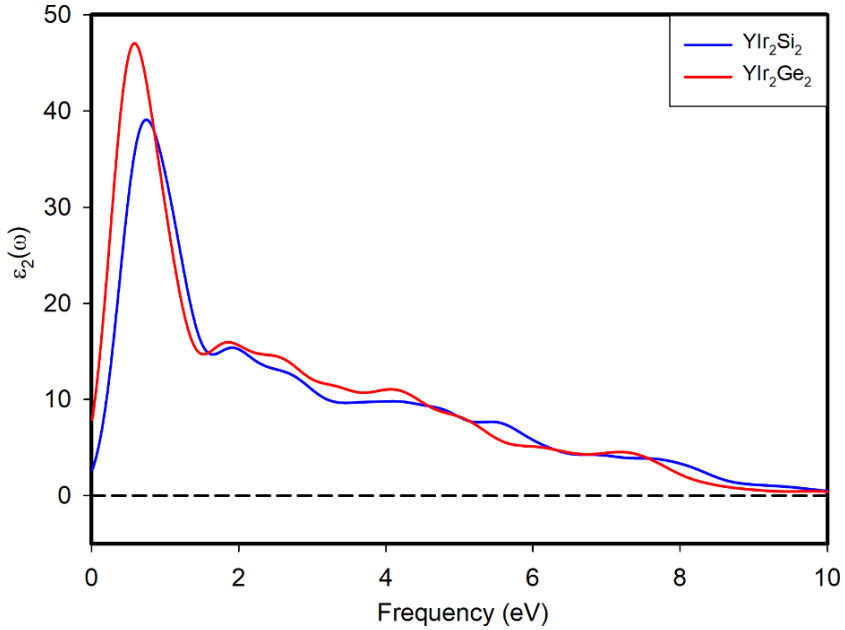

Figure 4. The imaginary part $\varepsilon_2(\omega)$ of dielectric function of YIr_2X_2 (X=Si, Ge).

The behavior of $\varepsilon_1(\omega)$ and $\varepsilon_2(\omega)$ are rather similar for these compounds with some differences in details. The main peaks of the real part for YIr_2X_2 (X=Si, Ge) occur at 0.22 and 0.19 eV, respectively. The same peaks reduce due to the interband transition and approach the minimum at about 1.8 eV for each compound. An important characteristic of $\varepsilon_1(\omega)$ is the zero-frequency

limit $\varepsilon_1(0)$, which is the electronic part of the static dielectric constant. For YIr_2X_2 (X=Si, Ge), static dielectric constant $\varepsilon_1(0)$ are found to be 52.26 and 72.68.

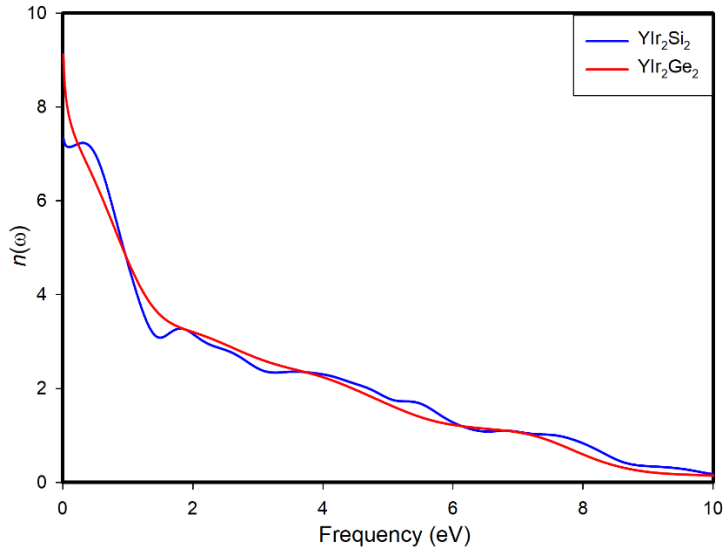

Figure 5. The Refractive index $n(\omega)$ of YIr_2X_2 (X=Si, Ge).

For the imaginary part of the dielectric function of YIr_2X_2 (X=Si, Ge), the absorption starts at about 0.73 eV and 0.57 eV, respectively. These points are due to G_v–G_c splitting, which gives the threshold for direct optical transitions between the absolute valence band maximum and the first conduction band minimum. This is known as the fundamental absorption edge [21].

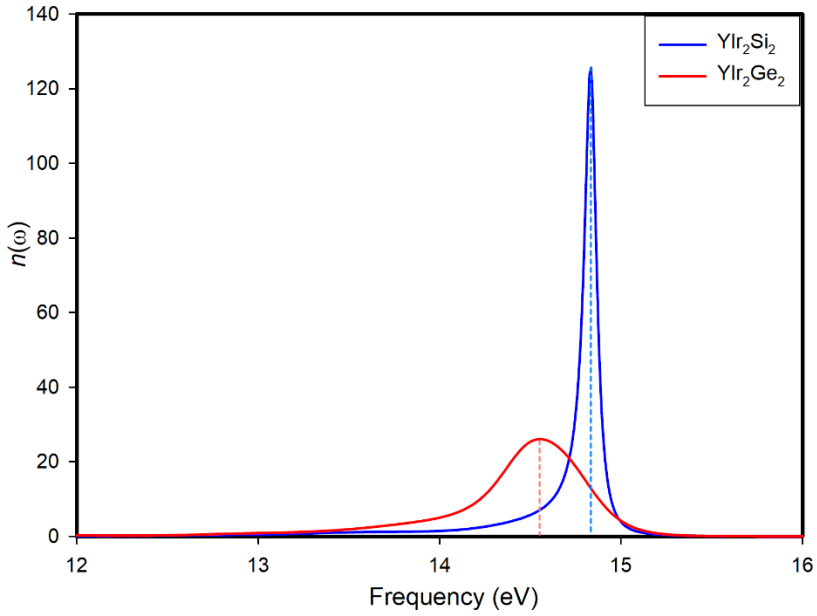

Figure 6. The Loss Function $L(\omega)$ of YIr_2X_2 (X=Si, Ge).

The dispersion curves ($n(\omega)$) for YIr_2X_2 (X=Si, Ge) are plotted in Fig. 5 and the values of refractive index $n(0)$ are found as 7.2 and 8.4, respectively. Finally, from the real and imaginary parts of the complex dielectric response function, the electron energy-loss function can easily

be obtained. It is the imaginary part of the reciprocal of the complex dielectric function, and its main peak so-called Plasmon frequency, above which the material exhibits the dielectric behavior while below which the material behaves like metallic. Our results are displayed in Fig. 6. The energy loss spectra do not show any distinct maxima in the range of about 0–13 eV. The reason for this is that the imaginary part of the dielectric function is still large at these energy values [19]. In the range of 13–16 eV, there are some large peaks in the energy loss spectra. At such high energies, the imaginary part of the dielectric function is small and the amplitude of the energy loss function becomes large. We have calculated the Plasmon frequency to be 14.85 and 14.53 eV, respectively. The composition dependence of the Plasmon frequency does not show a regular changing.

3.3. Phonon Dispersion Curves

The GGA phonon frequencies of YIr_2X_2 (X=Si, Ge) compounds are investigated by using the forces based on the CASTEP package. The code calculates force constant matrices and phonon frequencies using the "finite displacement method" [22]. Specifically, the phonon dispersion curves are calculated in high symmetry directions using a 2x2x2 cubic supercell of 80 atoms. The obtained phonon dispersion curves for these compounds along the high symmetry directions are shown in Fig. 7. Although some works were performed on the structural and elastic properties of these compounds, no experimental or other theoretical works exist on the lattice dynamics for comparison with our results.

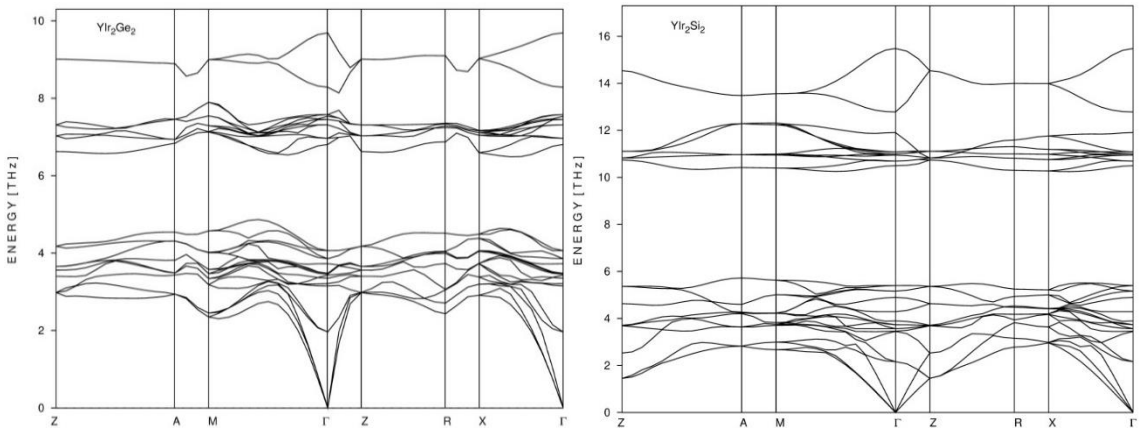

Figure 7. Calculated phonon dispersion curves for YIr_2X_2 (X=Si, Ge) Polymorphs.

The phonon frequency have a gap (approximately 4.5 THz and 1.7 THz, respectively) within optical branches is observed for YIr_2Si_2 and YIr_2Ge_2. The LO and TO branches have crossed between at Γ and X symmetry points. Also, the maximum values of the phonon frequencies for acoustic and optical branches decrease on going from Si to Ge atom.

3.4. Thermodynamic Properties

The results of a calculation of phonon dispersion can be used to compute internal energy (E), entropy (S), free energy (F), and heat capacity (C_v) as functions of temperature in the CASTEP code [9]. In this paper, the lattice dynamical contributions to the thermodynamic properties are evaluated to compute E, S, F, and C_v in the temperature range 0-1000 K. The quantities are calculated by the following relations [22]:

$$E(\mathrm{T}) = \mathrm{E}_{\omega t} + E_{zp} + \int \frac{\hbar\omega}{\exp\left(\frac{\hbar\omega}{kT}\right)-1} F(\omega)\,\mathrm{d}\,\omega \tag{6}$$

$$S(\mathrm{T}) = \mathrm{k}\left\{\int \frac{\frac{\hbar\omega}{kT}}{\exp\left(\frac{\hbar\omega}{kT}\right)-1} F(\omega)\,\mathrm{d}\,\omega - \int F(\omega)\left[1-\exp\left(-\frac{\hbar\omega}{kT}\right)\right]d\omega\right\} \tag{7}$$

$$F(\mathrm{T}) = \mathrm{E}_{\mathrm{tot}} + \mathrm{E}_{\mathrm{zp}} + \mathrm{kT}\int F(\omega)\ln\left[1-\exp\left(-\frac{\hbar\omega}{kT}\right)\right]d\omega \tag{8}$$

$$C_v(\mathrm{t}) = k\int \frac{\left(\frac{\hbar\omega}{kT}\right)^2 \exp\left(\frac{\hbar\omega}{kT}\right)}{\left[\exp\left(\frac{\hbar\omega}{kT}\right)-1\right]^2} F(\omega)\,\mathrm{d}\,\omega \tag{9}$$

where E_{zp} the zero-point energy, k is Boltzmann's constant, $\hbar$ is Planck's constant and $F(\omega)$ is the phonon density of states. The relationship between E, S, F, C_v and temperature are shown in Figs. 8-9 for YIr_2X_2 (X=Si, Ge) polymorphs, respectively. It is clear that the four thermodynamic properties increase linearly with temperature for these compounds.

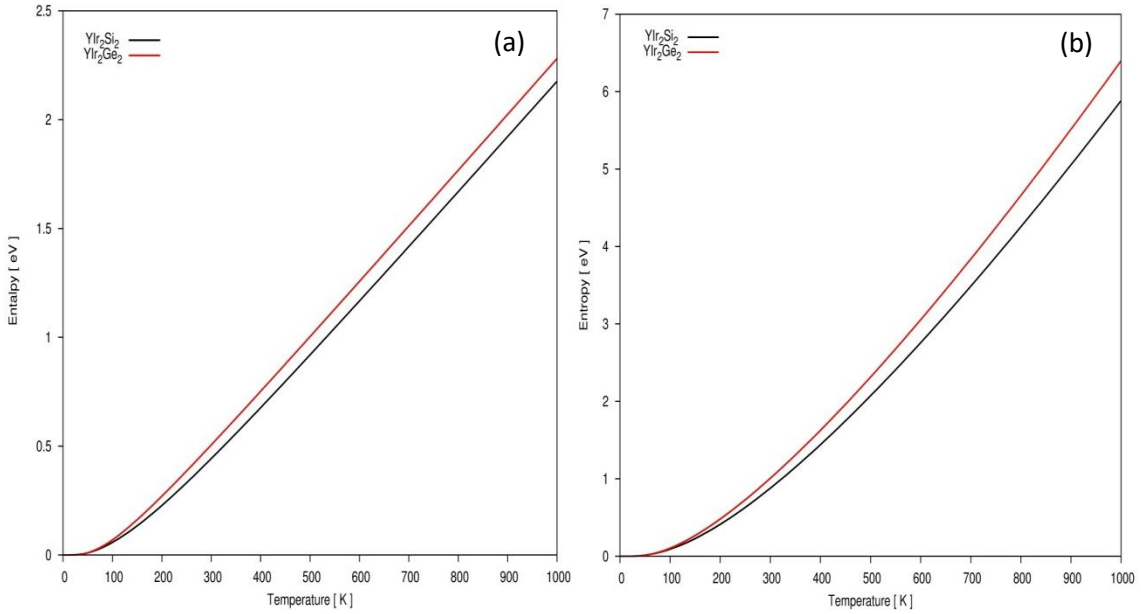

Figure 8. The variation of Entalpy and Entropy with temperature for YIr_2X_2 (X=Si, Ge) polymorphs.

From Fig. 9b, it can be concluded that, when T<500 K, C_v increases significantly with temperature, whereas the increase is slower for T>500 K. Thus, C_v approaches a constant known as the Dulong–Petit limit at higher temperatures for these compounds.

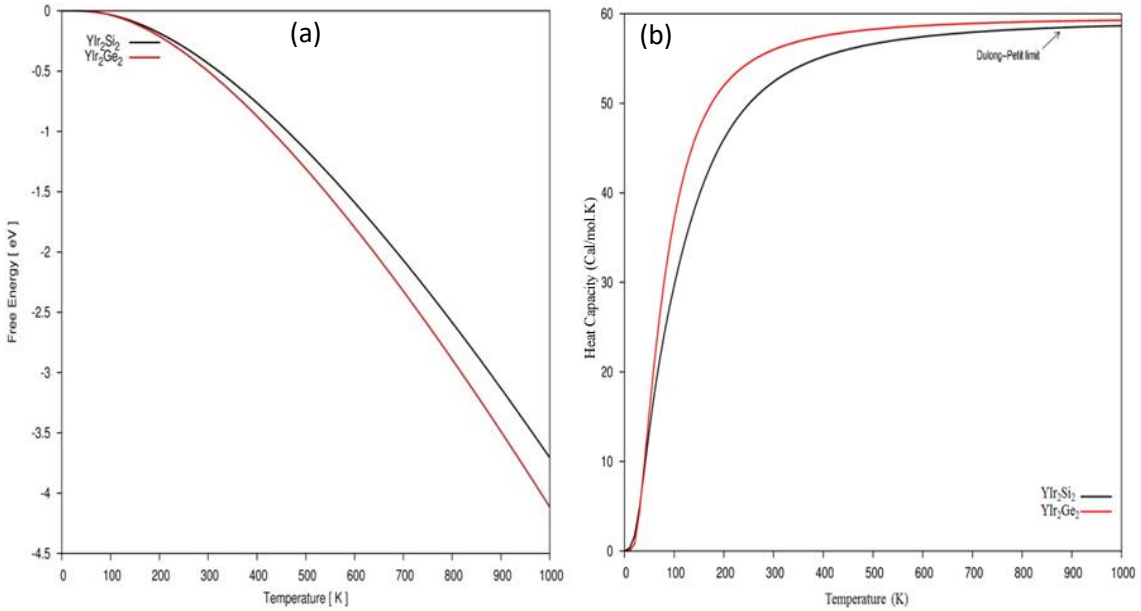

Figure 9. The variation of Free Energy and Heat capacity with temperature for YIr_2X_2 (X=Si, Ge) polymorphs.

4. CONCLUSIONS

In summary, we present the electronic, optical and lattice-dynamical properties of the YIr_2X_2 (X=Si, Ge) polymorphs, using the first-principles methods. Specifically, the lattice constants, dielectric function, refractive index, loss function and the tehrmodynamic constants are calculated, and results consistent with existing literature are obtained. The optical properties of this compounds are presented in detail. We anticipate that th eobtained results for dielectric constant, refractive index and Fermi levels for the first time in this work will be both experimentally validated in the future.

ACKNOWLEDGMENT

This work was supported by the Turkish Prime Ministry State Planning Agency under project no. 2011K120290.

References

[1] M. Vališka, J. Pospíšil, J. Prokleška, M. Diviš, A. Rudajevová, and V. Sechovský, *Journal of the Physical Society of Japan*, 81 (10) (**2012**) 104715.

[2] I.R. Shein and A.L. Ivanovskii, *Intermetallics*, 26 (**2012**) 1-7.

[3] I.R. Shein, *Physica B*, 406 (**2011**) 3525–3530.

[4] I.R. Shein and A.L. Ivanovskii, *Phys. Rev. B*, 83 (**2011**) 104501.

[5] V.V. Bannikov, I.R. Shein, A.L. Ivanovskii, *Physica B*, 407 (**2012**) 271–275.

[6] I.R. Shein and A.L. Ivanovskii, *Phys. Rev. B*, 84 (**2011**) 184509.

[7] I.R. Shein and A.L. Ivanovskii, *J Supercond Nov Magn*, 25 **(2012)** 151–154.

[8] E.D. Billington, S.A. Nickau, T. Farley, J.R. Ward, R.F. Sperring, T.E. Millichamp, and S.B. Dugdale, *Journal of the Physical Society of Japan*, 83(4) (**2014**) 044710.

[9] M.D. Segall, P.J.D. Lindan, M.J. Probert, C.J. Pickard, P.J. Hasnip, S.J. Clark, M.C. Payne, *J. Phys.: Condens. Matter*, 14 (11) (**2002**) 2717.

[10] T.H. Fischer, J. Almlof, *J. Phys. Chem.*, 96 (**1992**) 9768.

[11] J.P. Perdew, K. Burke, M. Ernzerhof, *Phys. Rev. Lett.*, 77 (**1996**) 3865.

[12] N. Troullier, J.L. Martins, *Phys. Rev. B*, 43 (**1993**) 1991.

[13] H.J. Monkhorst, J.D. Pack, *Phys. Rev. B*, 13 (**1976**) 5188.

[14] J.H. Xu, T. Oguchi and A.J. Freeman, *Phys. Rev. B*, 35 (**1987**) 6940.

[15] J.H. Xu and A.J. Freeman, *Phys. Rev. B*, 40 (**1989**) 11927.

[16] J. Sun, H.T. Wang and N.B. Ming, *Appl. Phys. Lett.*, 84 (**2004**) 4544.

[17] Y. Shena and Z. Zhou, *J. Appl. Phys.*, 103 (**2008**) 074113.

[18] M. Dadsetani and A. Pourghazi, *Phys. Rev. B*, 73 (**2006**) 195102.

[19] F. Wooten, *Optical Properties of Solids* (Academic, New York, 1972).

[20] N. Korozlu, K. Colakoglu and E. Deligoz, *J. Phys.: Condens. Matter*, 21 (**2009**) 175406.

[21] R. Khenata, A. Bouhemadou, M. Sahnoun, A.H. Reshak, H. Baltache and M. Rabah, *Comput. Mater. Sci.*, 38 (**2006**) 29.

[22] B. Montanari, N.M. Harrison, *Chem. Phys. Lett.*, 364 (**2002**) 528-534.

[23] S. de Gironcoli, S. dal Corso, A. Giannozzi, *P. Rev. Mod. Phys.*, 73 (**2001**) 515-562.